Hsi, J. P., Carter, J. P. & Small, J. C. (1994). *Géotechnique* **44**, No. 3, 381–396

Surface subsidence and drawdown of the water table due to pumping

J. P. HSI,* J. P. CARTER* and J. C. SMALL*

A fully coupled numerical method is presented for the analysis of the pumping of groundwater, taking into account the drawdown of the water table. The surface subsidence due to pumping is first studied assuming that the water table is not lowered as the groundwater is withdrawn. This solution is then compared with the solution for the case in which the drawdown of the water table is considered. Extensive parametric studies were carried out to provide non-dimensionalized design charts for surface subsidence and drawdown of the water table due to pumping.

KEYWORDS: consolidation; finite elements; groundwater; pore pressures; settlement.

L'article présente une méthode numérique permettant d'analyser le pompage des eaux souterraines en prenant en compte le rabattement de la surface libre de la nappe. La subsidence en surface du sol, due au pompage, est étudiée en supposant que la surface piézomètrique ne baisse pas au fur et à mesure que l'eau est pompée. Cette solution est ensuite comparée à la solution obtenue avec un rabattement de la surface piézomètrique. Des études paramètriques extensives ont été réalisées pour obtenides abaques adimensionnels donnant la subsidence de la surface du sol et le rabattement de la nappe dûs au pompage.

INTRODUCTION

It is a common practice to extract water from the ground for domestic, agricultural or industrial uses or to lower the groundwater level for construction work. Many historical cases have shown that such an exercise may cause significant surface subsidence (e.g. Scott, 1978; Delfranche, 1978; Premchitt, 1979; Harada & Yamanouchi, 1983; Hsi & Small, 1992a). The reason for this is that when the groundwater is withdrawn, the pore-water pressure reduces; also, the water table is lowered and so there is an increase in effective stress, causing consolidation of the layer of soil. This surface subsidence is of interest in geotechnical engineering, as excessive settlement in the vicinity of a pumped well may cause damage to surface structures or render them unserviceable. Therefore, an accurate prediction of ground settlement is sometimes crucial when groundwater is pumped.

Some solutions have been obtained for the prediction of how the groundwater table will fall as a result of pumping (e.g. Herbert, 1968; Taylor & Luthin, 1969; Neuman & Witherspoon, 1971; Rushton & Redshaw, 1979). However, these solutions do not include predictions of the surface deformation. Solutions for the pore-pressure changes obtained from such analyses have generally been used to predict surface settlements in conjunction with a deformation analysis, but such analyses are uncoupled, since the pore-pressure and deformation analyses are carried out separately (e.g. Gambolati & Freeze, 1973; Gambolati, Gatto & Freeze, 1974; Harada & Yamanouchi, 1983).

Some approaches for the prediction of surface subsidence due to pumping consider only the effect of reductions in pore pressure in the soil for the case where the phreatic surface remains unchanged (Booker & Carter, 1984, 1986a, 1986b, 1987; Small & Booker, 1984; Booker, Carter & Small, 1985; Kanok-Nukulchai & Chau, 1990). These solutions have generally been obtained by analytic or semi-analytic techniques. However, pumping will often draw down the water table, significantly affecting the distribution of the pore-water pressure, and so these analyses of subsidence may not be satisfactory in practice.

In this Paper a fully coupled numerical solution to the pumping problem is obtained. The method takes account of both the effects of the pore-pressure changes on the deformation of the soil and the effects of the deformation of the soil on the pore pressures, as well as the drawdown of the water table. Better predictions of surface subsidence are expected with the proposed coupled method because the effects of pumping are more accurately simulated; for the uncoupled methods already mentioned, soil deformation and drawdown of the water table are calculated separately.

Manuscript received 22 March 1993; accepted 28 June 1993.
Discussion on this paper closes 1 December 1994; for further details see p. ii.
* University of Sydney, Australia.

In this coupled analysis, flow is considered in both the saturated and unsaturated zones. Reduced flow in the unsaturated zone is simulated by reducing the permeability based on a simplified linear permeability–pore pressure relation. Deformation of the soil is calculated for the entire soil domain, including both saturated and unsaturated zones. However, when soil becomes unsaturated as the water table drops, pore suction is usually generated in this region. In reality, this suction may develop only up to a small limit value, depending on the type of soil. To account for this effect, in the analysis the pore suction must be limited to a specified upper bound. In this way, the soil deformation in the unsaturated zone can be calculated more realistically. The permeability–pore pressure relation and the limiting pore suction can be selected from experimental data for any particular soil (see Bouwer, 1964); however, typical values are used in the charts in this Paper.

Examples are given here for two separate cases: where the water table remains fixed and where it drops as a result of pumping. Numerical solutions for the case of no drawdown are verified by previous analytic solutions (Booker & Carter, 1984) and are then compared with solutions that allow the water table to be lowered. Non-dimensionalized design charts are included to allow an estimation of ground surface deformation and drawdown of the water table likely to be caused by pumping of groundwater.

COUPLED PROBLEM

The fully coupled numerical method, which has been developed for the analysis of ground surface subsidence due to pumping considering drawdown of the water table, involves theories of consolidation (Biot, 1941, 1956; Sandhu & Wilson, 1969; Christian & Boehmer, 1970; Hwang, Morgenstern & Murray, 1971; Small, Booker & Davis, 1976), transient unconfined seepage (Desai, 1976; Bathe, Sonnad & Domigan, 1982; Desai & Li, 1983) and pumping of groundwater (Taylor & Luthin, 1969; Neuman & Witherspoon, 1971; Rushton & Redshaw, 1979; Booker & Carter, 1984, 1986a, 1986b, 1987). This particular coupled problem has been studied by Hsi & Small (1992a, 1992b, 1992c, 1992d) who also give details of the development of the theory Hsi & Small (1992b) and Hsi (1992).

Theory

The analysis for a consolidating soil used in this study is based on Biot's equations (Biot, 1941, 1956), which assume that

(*a*) the soil is saturated (at least beneath the water table)
(*b*) the stresses are in equilibrium
(*c*) the effective stresses and strains obey Hooke's law
(*d*) the flow is governed by Darcy's law
(*e*) the pore water and soil solids are incompressible
(*f*) volume change within the soil corresponds to the expulsion of an equivalent volume of pore fluid
(*g*) the deformations of the soil skeleton are small.

In practice, it is often necessary to solve Biot's equations numerically. Some numerical approaches have been developed by Sandhu & Wilson (1969), Christian & Boehmer (1970), Hwang *et al.* (1971), Small *et al.* (1976) and Hsi & Small (1992b). In this particular problem involving drawdown of the water table, the time marching scheme (α integration rule) proposed by Small *et al.* (1976) and the iterative incremental form proposed by Hsi & Small (1992b) were used in the solution procedure.

The residual flow procedure proposed by Desai & Li (1983) and Bathe *et al.* (1982) is used to account for the drawdown of the water table. The concept of this procedure is that when the water table falls from a previous position to the present one, the water initially stored in the pores of the soil in the zone between these two positions is released, and this amount of water needs to be imposed as a flow across the present free surface. When this is done, a new location of the free surface, which is also a zero pore-pressure contour, can be determined. The essence of this solution procedure is that the finite element mesh remains unchanged and the free surface is allowed to pass through the elements. The terms water table and free surface in this Paper both refer to the surface along which the pore-water pressure equals the atmospheric pressure. Following the usual convention, atmospheric pressure is adopted as zero for the pore-pressure measurement.

Governing equations

The finite element equations used to obtain an approximate solution to the coupled problem of pumping of groundwater involving drawdown of the water table can be written as

$$\begin{bmatrix} \mathbf{K} & -\gamma_w \mathbf{L}^T \\ -\gamma_w \mathbf{L} & -\gamma_w(1-\alpha)\Delta t\boldsymbol{\Phi} - \gamma_w \mathbf{G}^{FS} \end{bmatrix} \begin{bmatrix} \Delta\boldsymbol{\delta}^{(i)} \\ \Delta\boldsymbol{h}^{*(i)} \end{bmatrix} = \boldsymbol{\zeta} \quad (1)$$

where

$$\zeta = \begin{bmatrix} \Delta f^{(i)} \\ \gamma_w \alpha \Delta t \mathbf{\Phi} \boldsymbol{h}_t^* + \gamma_w (1-\alpha) \Delta t \mathbf{\Phi} \boldsymbol{h}_{t+\Delta t}^{*(i-1)} \\ -\gamma_w \mathbf{L} \boldsymbol{\delta}_t + \gamma_w \mathbf{L} \boldsymbol{\delta}_{t+\Delta t}^{(i-1)} \\ +\gamma_\omega \mathbf{G}^{FS} (\boldsymbol{h}_{t+\Delta t}^{*(i-1)} - \boldsymbol{h}_t^*) + \gamma_\omega \Delta t \boldsymbol{Q} \end{bmatrix} \quad (2)$$

All the terms used here are defined in Appendix 1 and Notation: details of their derivation are given by Hsi & Small (1992b) and Hsi (1992).

Equations (1) and (2) can be solved for nodal displacements $\boldsymbol{\delta}$ and total water heads $\boldsymbol{h}^*$. As the free-surface boundary in the pumping problem (see Fig. 1) changes while the water table is falling, iterations (denoted as i) at each time-step (denoted as t) are necessary in the solution procedure until convergent results are obtained.

In these equations, the terms containing $\mathbf{G}^{FS}$ arise from the water released by the soil due to the fall of the water table, and the total water head $\boldsymbol{h}^*$ in these terms is the head along the free surface. These terms impose flows at the nodes of the elements through which the free surface passes. The term $\mathbf{G}^{FS}$ is given by

$$\mathbf{G}^{FS} = \int_\Gamma \mathbf{a}\mathbf{a}^T S_y \cos\beta \, d\Gamma \quad (3)$$

where S_y is the specific yield of the soil (sometimes known as the effective porosity). S_y (volume of water per unit volume of soil) determines the amount of water that the soil can yield from storage within the zone between the previous and the present positions of the free surface. $\boldsymbol{a}$ is the vector of shape functions for pore pressure and head, β is the angle between the horizontal direction and a segment of the free surface, and Γ is the free surface contour.

Along the free surface, the total water head is equal to the elevation head; this can be written as

$$h^* - h_{EL} = \sum_{j=1}^{m} N_j(\xi, \eta)(h_j^* - h_{EL,j}) = 0 \quad (4)$$

where m is the number of nodes attached to an element; $N_j(\xi, \eta)$ is the shape function for the head at node j, h_j^* and $h_{EL,j}$ are the total water head and elevation head at node j, and (ξ, η) are local co-ordinates. From equation (4), the local co-ordinates (ξ, η) along the free surface can be found, and hence the global co-ordinates (x, y) can be evaluated by the usual methods. Given these co-ordinates, the integration along the free surface in equation (3) can be approximated by a summation.

In the pumping operation, the pumping rate Q (volume of water per unit time) is assumed to be constant from time t to $t + \Delta t$. The term containing the vector of pumping rates $\boldsymbol{Q}$ in the governing equations represents the extraction of water from the ground and is applied directly to the nodes from which the water is pumped.

The numerical procedure described here does have limitations. In particular, the value assigned to the pumping rate Q can significantly influence the results of the analysis. If a large pumping rate is specified, a significant zone of negative pore pressure will be predicted around the sink. The numerical analysis should be stable if this zone of negative pore pressures remains distinct from the region of negative pore-water pressures above the water table. However, the numerical procedure will no longer be valid if the two regions become contiguous, i.e. if the pumping rate is large enough to cause the water table to be drawn down close to the level of the sink.

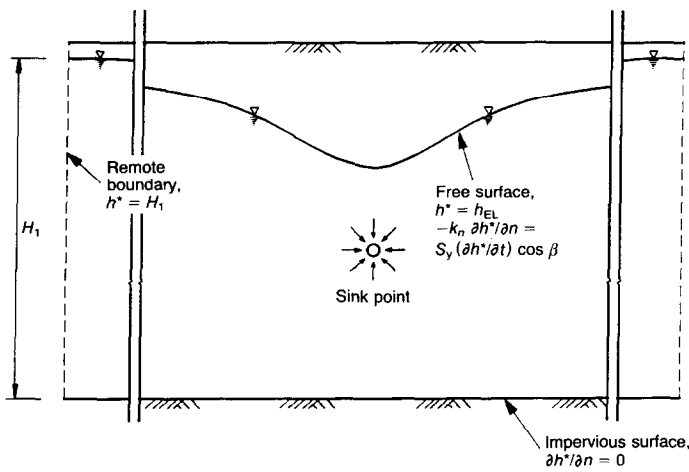

Fig. 1. Boundary conditions for the pumping problem

Permeability–pore pressure relation

As the water table drops, the soil above the free surface becomes unsaturated and so reduced flow occurs in this region. To model this small flow, the permeability of the soil above the free surface is reduced. However, regions with large differences in permeability have the potential to cause instabilities in the numerical solution. Furthermore, when a coupled problem is being solved, compressibility of the soil can significantly influence the convergence of the solution process. Two measures are adopted here to overcome the potential for numerical instability.

(*a*) The reduction of the permeability above the free surface follows a continuous permeability k–pore pressure P relation (Bouwer, 1964; Freeze, 1971; Cathie & Dungar, 1975; Desai & Li, 1983), as shown in Fig. 2. The permeability reduces linearly with the pore pressure when the latter becomes negative, and a limiting value of pore pressure P_{limit} is assigned at which the permeability is given a very small constant value k_{limit}.

(*b*) The permeabilities of the elements through which the free surface passes are not reduced immediately because the flow of the stored fluid released due to the fall of the free surface is imposed at the nodes of these elements.

In the unsaturated zone above the free surface, it is necessary not only to reduce seepage by lowering the permeability, but also to control the pore pressures as they influence the deformation of the soil through the effective stress law. Usually some soil suction develops when the pores are at low levels of saturation, and for different types of soil, this suction has its limit (e.g. higher suctions can be reached for clays; sands usually sustain lower suctions). To calculate the deformations accurately for the soil in the unsaturated zone, this effect must be taken into account in the analysis. Here the limit pressure P_{limit} is chosen to correspond to the ultimate pore suction pressure. Once the pore pressures above the free surface reach this value they are maintained at the limit pressure. The prescribed limit pressures can be set at any desired values, which can be determined by experiments or by experience. Bouwer (1964) summarizes various experimental methods to determine the relation of the reduced permeability and the negative pore pressure, from which a simplified linear relation (see Fig. 2) and the limit pore suction P_{limit} can be obtained.

In a parametric study by Hsi (1992), it was found that the slope of the permeability–pore pressure relation has only a slight influence on the position of the free surface; however, it does affect the shape of the free surface. It was found that the steeper the slope, the greater is the curvature of the free surface, and the flatter the slope, the smaller is the curvature of the free surface. As the position of the free surface is not greatly affected by the permeability–pore pressure relation (or the limit pressure P_{limit}), the overall deformation of the soil is not affected significantly by this factor.

EXAMPLES AND COMPARISONS

Two examples of the pumping problem are presented here. In one, the position of the water table is considered to remain constant when the pumping is carried out (i.e. recharge occurs at the free surface); the other allows for drawdown of the water table. The numerical solution to the first example in which no drawdown is considered was verified by an analytic solution (Booker & Carter, 1984). The effect of drawdown of the water table on the surface subsidence is investigated by comparison of the two numerical solutions.

Pumping without drawdown of the water table

This problem consists of a point sink located at depth h within a porous soil deposit of thickness H, as shown in Fig. 3. As the numerical solution

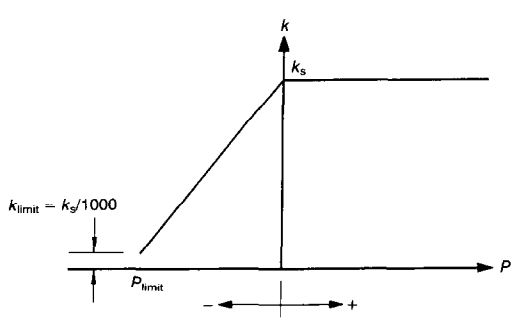

Fig. 2. Permeability–pore pressure relation

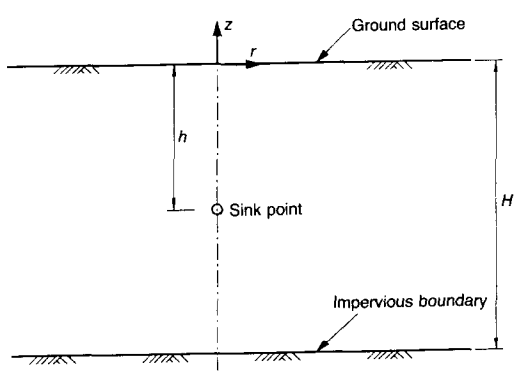

Fig. 3. Problem definition

is to be verified by comparison with an analytic solution (Booker & Carter, 1984) which assumes that the point sink is embedded in a poro-elastic half space, a large H/h ratio is needed for the numerical analysis.

To simulate this problem, the soil parameters chosen for the analysis were: Young's modulus $E' = 1 \times 10^5$ kPa, Poisson's ratio $v' = 0{\cdot}25$, permeability $k = 0.01$ m/day and the unit weight of water $\gamma_\omega = 10$ kN/m^3. The pumping rate Q was specified as 2 m^3/day. The embedded depth h of the sink point was selected to be 10 m, and the thickness H of the soil deposit was assumed to be 150 m in the numerical analysis. The problem was considered to be axially symmetric, and the finite element mesh shown in Fig. 4, which consists of 320 eight-noded isoparametric elements and 1033 nodes, was used for the analysis. The boundary conditions for the problem are also shown in Fig. 4.

Based on the study by Booker & Carter (1984), the non-dimensional time factor T_v is given by

$$T_v = ct/h^2 \tag{5}$$

where

$$c = (\lambda + 2G)k/\gamma_w \tag{6}$$

In equation (6), G is the elastic shear modulus, related to E' and v' by

$$G = E'/2(1 + v') \tag{7}$$

and the Lamé constant λ is given by

$$\lambda = 2Gv'/(1 - 2v') \tag{8}$$

To select values of the non-dimensional time factor T_v used in Fig. 7, the time-step sizes chosen for the analysis were 0·008$\dot{3}$, 0·08$\dot{3}$, 0·8$\dot{3}$, 83·$\dot{3}$, 833·$\dot{3}$, 8333·$\dot{3}$ and 833 333·$\dot{3}$ days, corresponding to $T_v = 0{\cdot}01$, 0·1, 1, 10, 100, 1000, 10 000 and 1 000 000 respectively.

The long-term (steady-state) surface settlement S_0 immediately above the sink (at $r = 0$) calculated by the numerical procedure was 0·1940 cm. The analytic solution for S_0 for a half-space problem is given by Booker & Carter (1986a) as

$$S_0 = \frac{Q\gamma_w}{4\pi k(\lambda + G)} \tag{9}$$

Based on equation (9), the calculated value of S_0 was 0·1989 cm. Hence the numerical solution agrees well with the exact result. A non-dimensionalized plot of surface subsidence S at transient and steady-state stages is shown in Fig. 5. The small discrepancies between the numerical and analytic solutions are probably due to the restraints imposed at the finite boundaries in the numerical analysis. The profiles of the non-dimensionalized excess pore pressures p (changes from the initial pore pressures) at various times along the vertical axis $r = 0$ are shown in Fig. 6, in which the numerical and analytic solutions agree reasonably well.

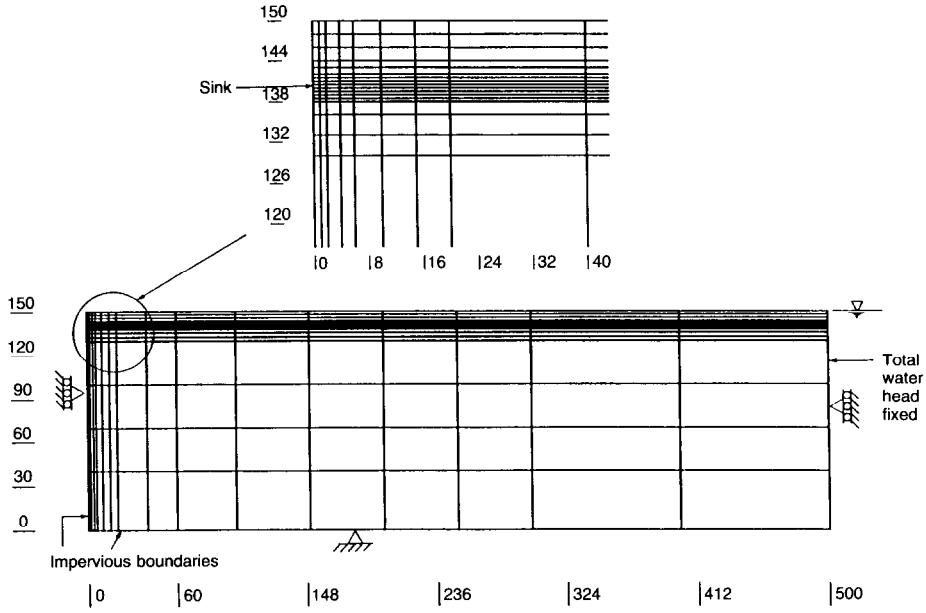

Fig. 4. Finite element mesh used for analysis

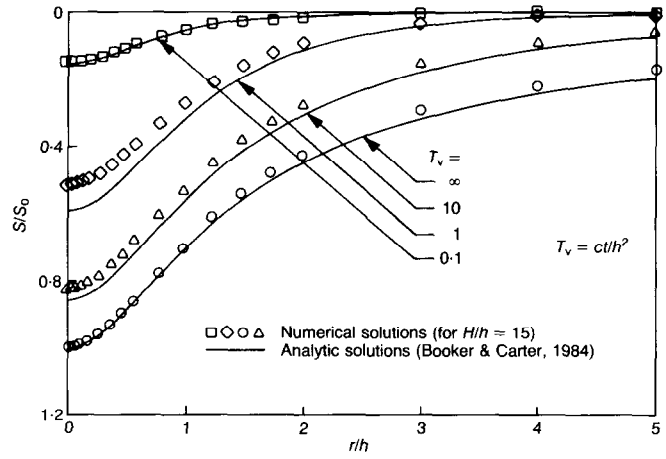

Fig. 5. Isochrones of surface subsidence: drawdown not considered

The ordinate shown in Fig. 5 is the ratio of surface settlement S to the long-term surface settlement S_0. For a later comparison when drawdown of the water table is taken into consideration, it is interesting to present the magnitude of the surface subsidence d_s. This is shown non-dimensionally on the left-hand side of Fig. 7.

Pumping with drawdown of the water table

The second example of pumping presented here allows for the drawdown of the water table. For the transient problem, it is the Authors' experience (Hsi & Small, 1992b; Hsi, 1992) that the solution has always been found to converge when the integration factor α used in equations (1) and (2) is chosen to be zero (implicit Euler backward method). Therefore the same mesh for this more difficult problem with a moving free surface boundary is still regarded as suitable, and is used for all the examples in this study. This example also used the same time-step sizes and soil parameters as were used in the previous example. In addition, the specific yield S_y must be specified in the analysis considering drawdown of the water table, and it was chosen to be 0·0083. The ultimate negative pore pressure P_{limit} above the free surface was specified as -20 kPa. Bouwer (1964) plotted permeability against pore pressure for various types of soil. Typical values of limit pressure P_{limit} can be obtained from these plots, in which P_{limit} varies from about -2 to -15 kPa for sands, -7 to -25 kPa for loams and -6 to -20 kPa for clays. Therefore, the value of P_{limit} chosen here for the analysis is considered to be a typical value for many soils and is used for all the

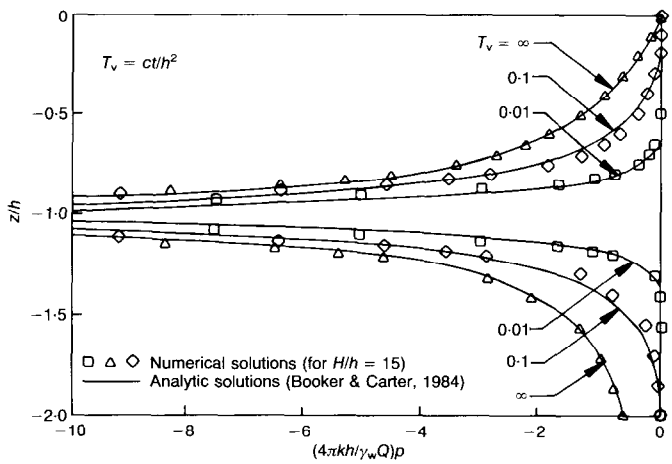

Fig. 6. Isochrones of excess pore pressure: drawdown not considered

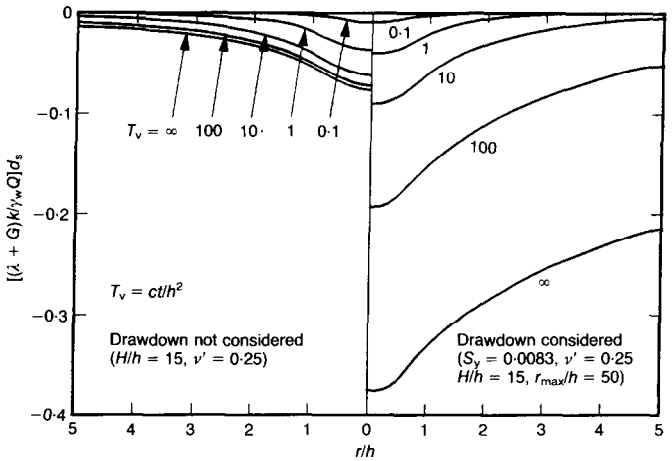

Fig. 7. Surface subsidence profiles

analyses in this study. However, the sensitivity of soil deformation and drawdown of the water table to changes in P_{limit} has been investigated. Another value, $P_{limit} = -50$ kPa, was used for the analysis of the same problem. It was found that nearly identical solutions for deformation and drawdown were obtained. This shows that the value of P_{limit} does not greatly affect the solutions discussed in this Paper, and so a fixed value ($P_{limit} = -20$ kPa) was used in all subsequent analyses.

Allowing for drawdown, the calculated long-term surface settlement at $r = 0$ was $S_0 = 0{\cdot}9305$ cm, which is about five times greater than the previous solution (without drawdown). The surface subsidence ratio S/S_0 is shown in Fig. 8. The shapes of these isochrones are very different from the ones shown in Fig. 5. The predicted subsidence is distributed much more widely when drawdown of the water table is included in the analysis. However, Figs 5 and 8 do not show the absolute magnitude of the settlement. To provide this information, a non-dimensionalized plot of the surface subsidence is also presented in Fig. 7. From a comparison of the two cases, with and without drawdown of the water table (Fig. 7), it is clearly seen that at most times the surface subsidence is much greater when drawdown of the water table is considered in the analysis.

The excess pore pressures along the vertical axis $r = 0$ are shown in Fig. 9. It was found that when the time factor is small (e.g. $T_v = 0{\cdot}01$ and 0·1) there is no significant drawdown of the water table, and so the excess pore-pressure isochrones at these stages are almost identical to those where no drawdown is allowed (compare Figs 6 and 9).

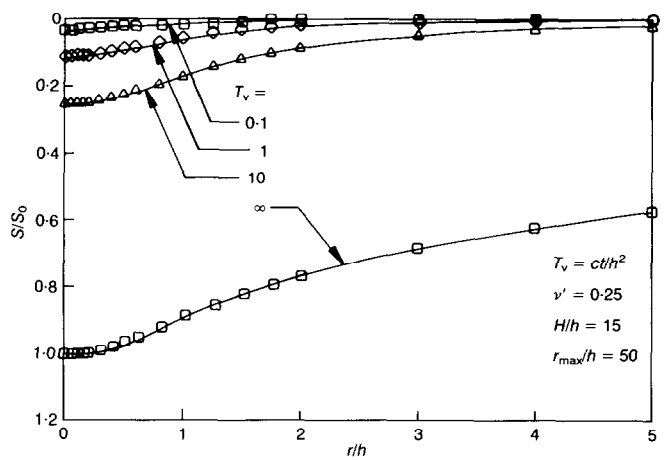

Fig. 8. Isochrones of surface subsidence: drawdown considered

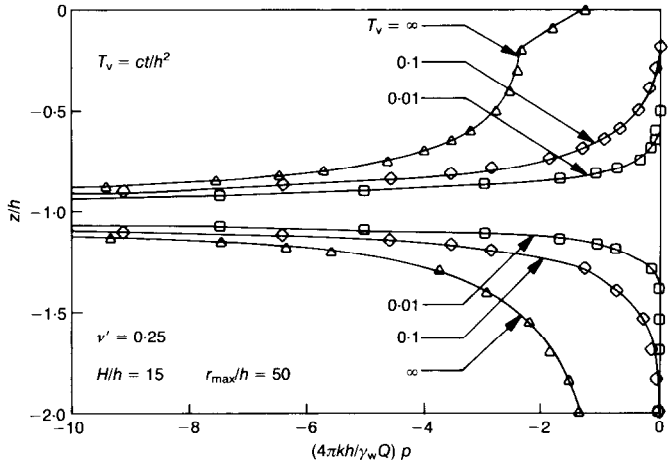

Fig. 9. Isochrones of excess pore pressure: drawdown considered

However, at larger times the pore-pressure distributions are quite different, as the drawdown of the water table becomes more important. This phenomenon is also seen in Fig. 7.

PARAMETRIC STUDIES AND DESIGN CHARTS

In an attempt to establish design charts for pumping problems, extensive parametric studies were carried out to find the major factors that affect the drawdown of the water table and the surface subsidence. The results of these studies are presented in non-dimensional form.

Drawdown of the water table

Through parametric studies, it has been found that the drawdown d_h* of the water table is closely proportional to $1/k$, $1/h$ (when H/h is constant) and Q. The transient positions of the water table were found to be affected by the value of S_y used in the analysis, but the steady-state position is not affected by this parameter. The Young's modulus E' and the Poisson's ratio ν' of the soil skeleton have a slight influence on the drawdown behaviour. The ratio H/h affects the drawdown solution significantly; this is discussed later.

For most of these studies, the outer boundary was always maintained at a distance r_{max} where $r_{max} = 50h$. Some case histories have shown that there is little drawdown of the water table at radial distances beyond about $20h$ from the location of the sink (Debidin & Lee, 1980; Taipei Civil Engineers' Association, 1985; Hsi & Small, 1992a). This is because in practice recharge of groundwater often occurs at some distance from the pump, and this maintains the groundwater table in this vicinity at its original level. As the condition of recharge varies from site to site, the ratio r_{max}/h was taken as 50 in this parametric study, to be conservative with respect to the calculated drawdown and the resulting settlements. The effect of this outer boundary is discussed later.

Transient and steady-state solutions for drawdown of the water table are shown non-dimensionally in Fig. 10, for which the ratio H/h is 15. In this plot, the non-dimensional time factor T_d was chosen to be

$$T_d = kt/S_y h \tag{10}$$

This is similar to the time factor chosen for a drawdown problem in a square dam presented by Bathe *et al.* (1982) and Herbert (1968).

As this numerical method is fully coupled, the drawdown of the water table can significantly affect the surface settlement and vice versa. Therefore the time factor T_d in non-dimensional plots of the drawdown of the water table should be used in association with the time factor T_v (see equation (5)) which was used previously in non-dimensional plots of the surface subsidence. It has been found that almost unique non-dimensionalized plots can be obtained when the ratio T_v/T_d remains constant. However, only the transient solutions depend on this ratio (i.e. the steady-state solutions are identical for all T_v/T_d ratios, as shown in Fig. 10).

It is not possible to obtain a unique plot for the drawdown of the water table from the coupled numerical analysis, as the drawdown effect is influenced marginally by other factors such as the elastic properties of the soil. However, Fig. 10 provides a satisfactory non-dimensionalization of the results with very small variations for a wide range of soil parameters. The ranges of the

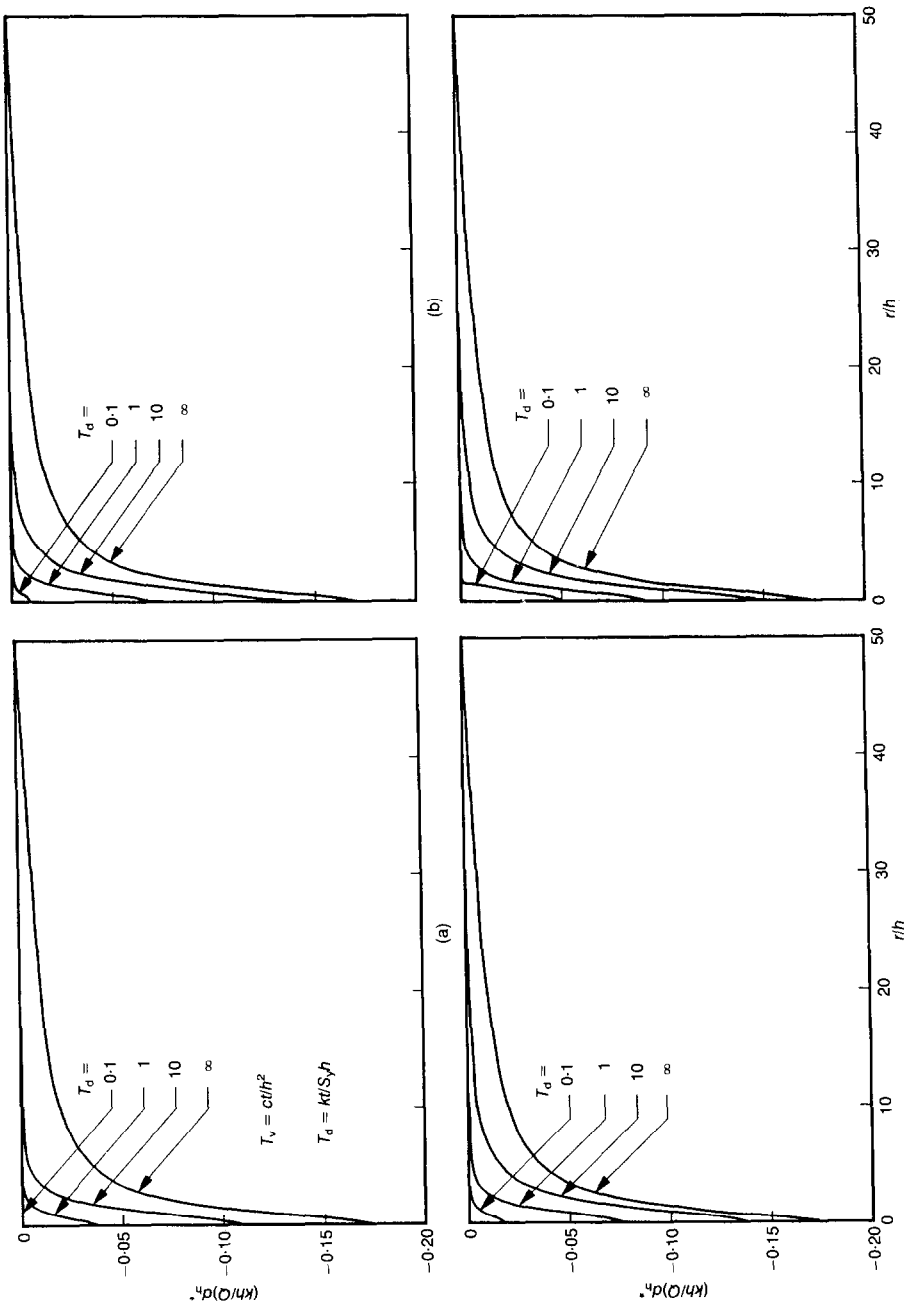

Fig. 10. Transient and steady-state drawdown profiles of the water table, $H/h = 15$, $r_{max}/h = 50$: (a) $T_v/T_d = 1$; (b) $T_v/T_d = 10$; (c) $T_v/T_d = 100$; (d) $T_v/T_d = 1000$

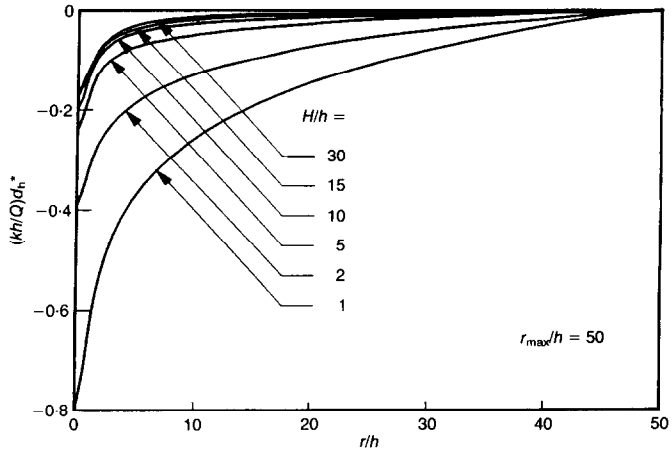

Fig. 11. Influence of H/h on steady-state drawdown profile

parameters used to test the non-dimensionalization were: Young's modulus $E' = 1 \times 10^3$ to 1×10^5 kPa, permeability $k = 1 \times 10^{-3}$–1×10^2 m/day, specific yield $S_y = 0{\cdot}001$–$0{\cdot}1$, and Poisson's ratio $\nu' = 0{\cdot}15$–$0{\cdot}45$. Random combinations of these parameters were chosen for the analysis, and nearly unique non-dimensional plots were obtained. The same ranges of parameters were used for the analysis of subsidence presented in the following section; again, the effect on the non-dimensional plots was found to be very small.

It is also interesting to see how the ratio of layer thickness to sink depth H/h affects the drawdown behaviour. Steady-state solutions for drawdown of the water table for various values of H/h are shown in Fig. 11. It is seen that the smaller the H/h value, the larger is the drawdown. This is because when H/h is lower, more water supplying the pump comes from the groundwater above the sink, and so greater drawdown is generated. A plot of the steady-state drawdown on the vertical axis $r = 0$ against H/h is shown in Fig. 12. It is seen that when H/h becomes large, the changes in drawdown become less significant as the impermeable boundary beneath the soil layer has less influence on the solution. When H/h is smaller than 5, the finite layer thickness has a much greater influence on the drawdown behaviour.

Figure 13 shows the influence of the outer boundary adopted in the finite element model on the final (steady-state) profile of the water table. At this outer boundary, it was assumed that the

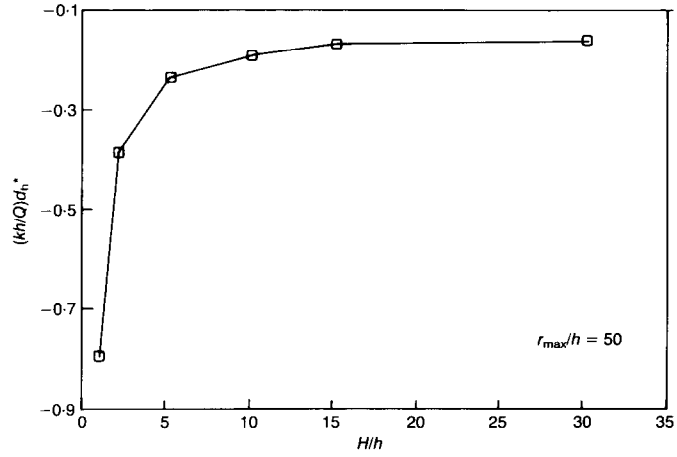

Fig. 12. Steady-state drawdown of the water table at $r = 0$ plotted against H/h

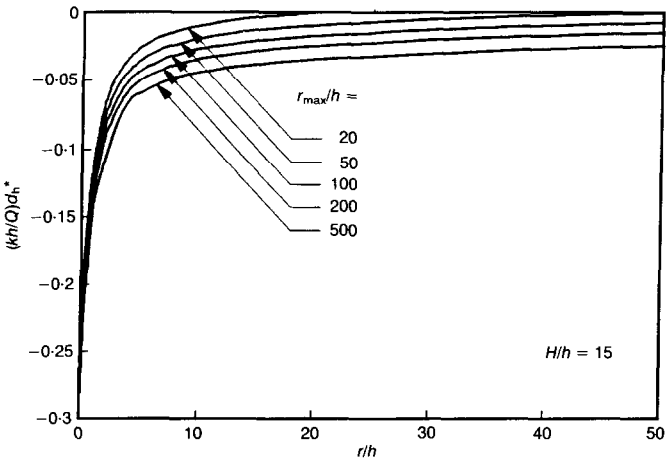

Fig. 13. Influence of r_{max}/h on steady-state drawdown profile

free surface remained at its original level, i.e. at the level of the soil surface. It is seen that the further away the boundary, the greater is the drawdown of the free surface. This is because by maintaining the water surface at its original level at the outer boundary, one is in effect supplying an inflow at this boundary to maintain the water level. The further away the boundary, the smaller is the influence of this recharge. In most field cases, there is recharge to the groundwater and this means that the water table will remain effectively at its original level at some finite distance from the pump. This distance was chosen to be $r_{max} = 50h$ for most of the study presented in this Paper.

Surface subsidence

The surface subsidence d_s has been found to be closely proportional to $1/E'$, $1/k$ and Q. The non-dimensional time factor T_v (as defined in equation (5)) was previously chosen for use in non-dimensional plots of surface subsidence when no drawdown occurred. However, the solutions for the surface settlement are closely related to the position of the free surface during drawdown, therefore the time factor T_v must be used in association with the time factor T_d (see equation (10)). Unique non-dimensionalized plots can again be obtained when the ratio T_v/T_d remains constant. However, only the transient solutions are affected by this ratio.

The transient and steady-state solutions for surface subsidence are presented non-dimensionally in Fig. 14 for T_v/T_d values of 1, 10, 100 and 1000. For these cases, H/h was chosen to be 15 and ν' was specified as 0·3.

Poisson's ratio ν' was found to have a small influence on the surface subsidence. The steady-state surface subsidence profiles for various Poisson's ratios (e.g. $\nu' = 0{\cdot}15$, 0·3 and 0·45) are shown in Fig. 15, where the predictions are seen to fall into a narrow band.

The steady-state surface subsidence profiles for various H/h values are shown in Fig. 16. The influence of the finite layer thickness is more pronounced close to the axis $r = 0$, as greater drawdown of the water table occurs near this axis. The maximum steady-state surface subsidence at $r = 0$ is plotted against H/h in Fig. 17. For a given pumping rate Q, when H/h becomes large the effect of changes in H/h on subsidence becomes small, and when H/h is less than 5 changes in the position of the lower boundary have a greater influence on the surface subsidence.

The influence of the ratio r_{max}/h on the solution for the steady-state subsidence is seen in Fig. 18. Larger settlements are predicted when the distance to the outer boundary is increased. This is because more drawdown occurs as the ratio r_{max}/h is increased, and so more consolidation of the soil is caused.

CONCLUSIONS

A fully coupled numerical method has been developed for the analysis of soil subsidence due to pumping of groundwater. This analysis can take account of the drawdown of the water table.

Examples of the influence of pumping have been given for cases with and without drawdown of the water table. Numerical solutions for the case where the water table does not drop were compared with the analytic solutions presented by Booker & Carter (1984). Reasonable agreement was found. However, the numerical analysis

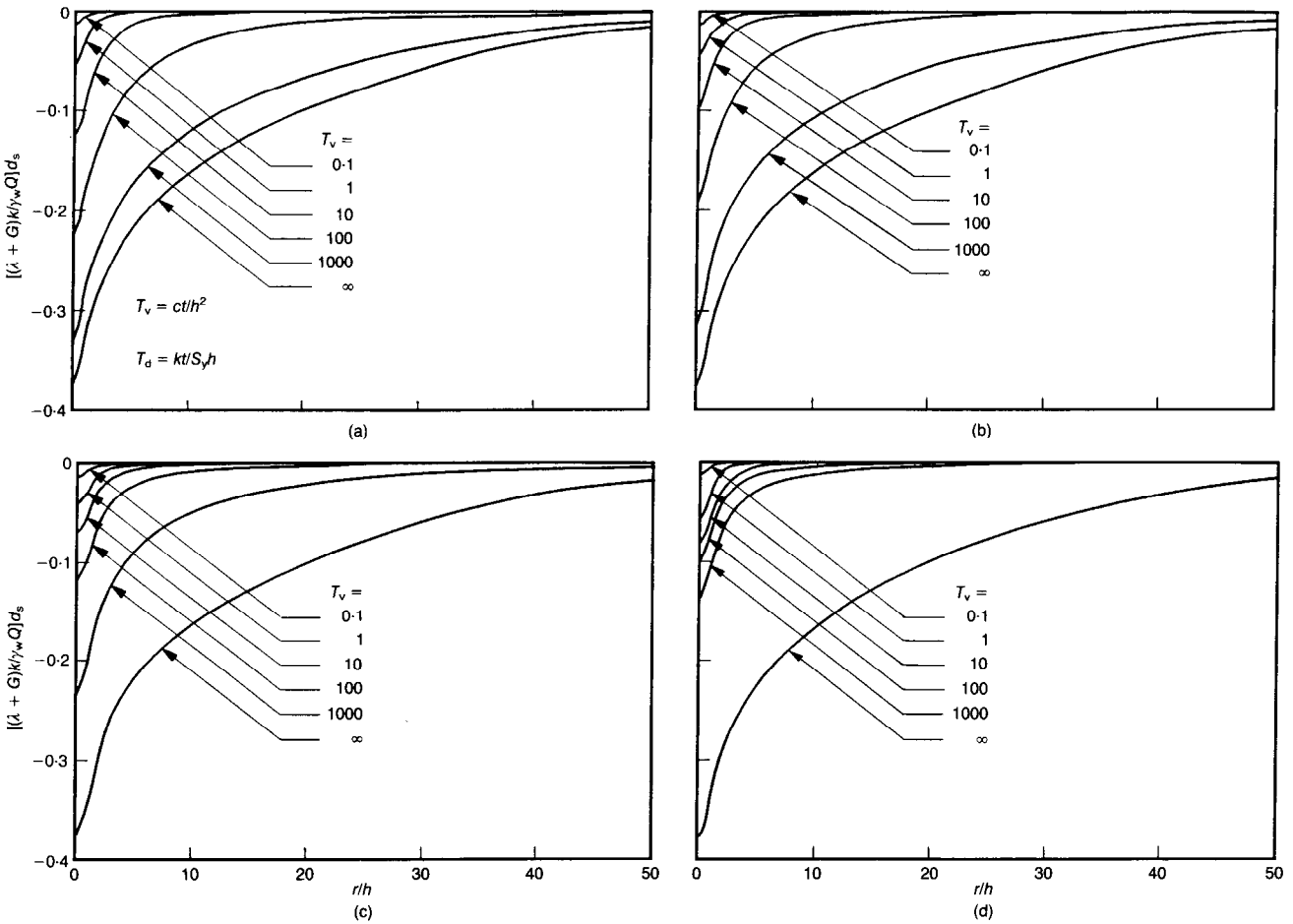

Fig. 14. Transient and steady-state solutions for surface subsidence profiles ($\nu' = 0.3$, $r_{max}/h = 50$, $H/h = 15$): (a) $T_v/T_d = 1$; (b) $T_v/T_d = 10$; (c) $T_v/T_d = 100$; (d) $T_v/T_d = 1000$

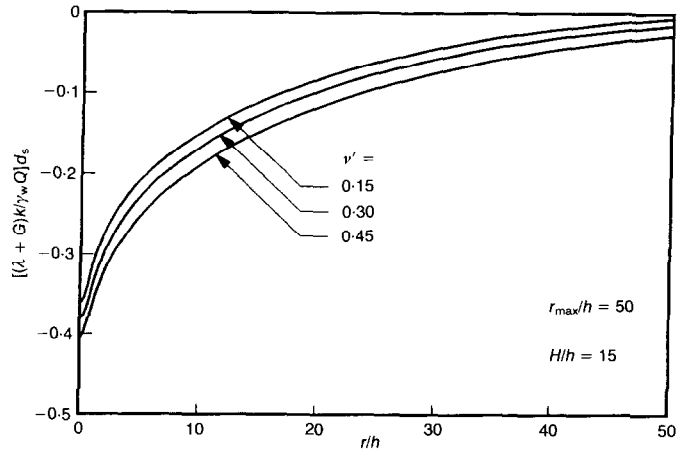

Fig. 15. Steady-state surface subsidence profiles for various values of Poisson's ratio

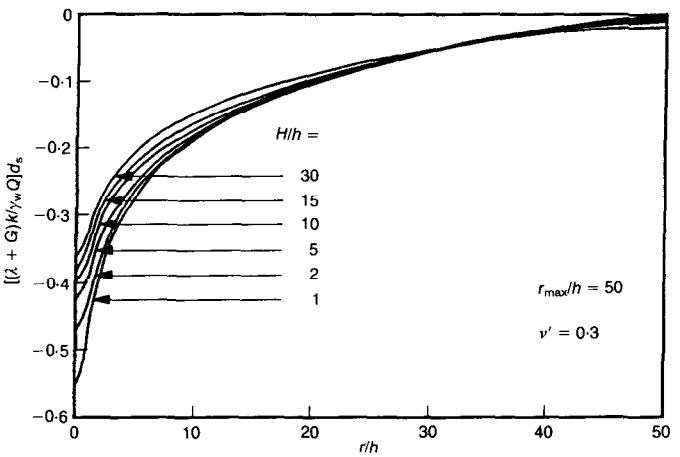

Fig. 16. Influence of H/h on steady-state surface subsidence profile

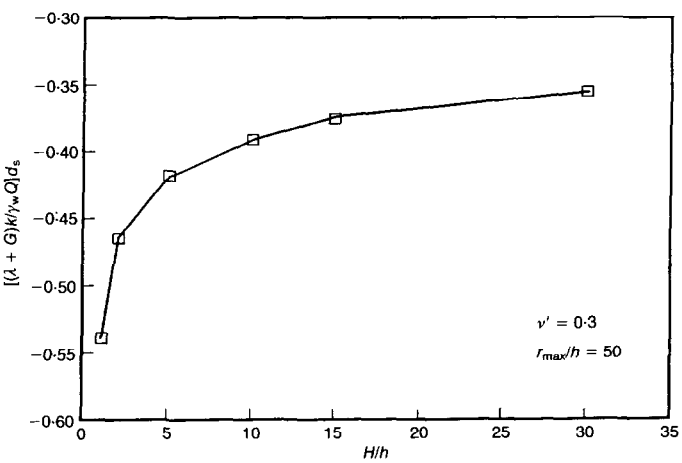

Fig. 17. Steady-state surface subsidence at $r = 0$ plotted against H/h

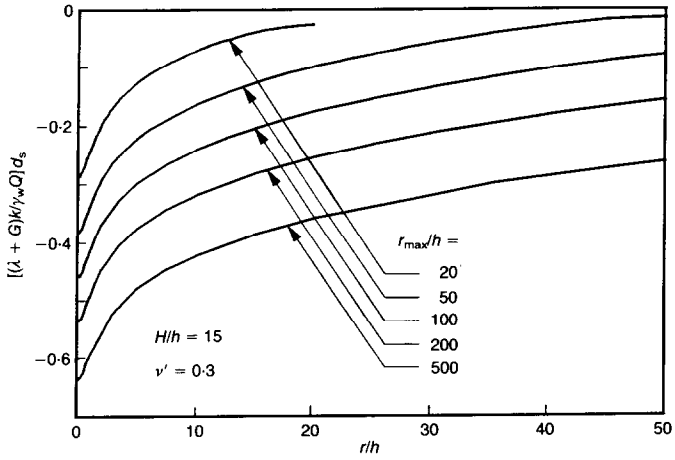

Fig. 18. Influence of r_{max}/h on steady-state surface subsidence profile

indicated that the drawdown of the water table has a significant effect on the pore-pressure distribution within the soil and the surface subsidence. Ignoring this effect could lead to gross underestimates of the subsidence.

Extensive parametric studies have allowed the preparation of design charts. Non-dimentionalized plots of the surface subsidence and drawdown of the water table are presented in these charts, which can be used to obtain rapid solutions to problems involving pumping of groundwater in uniform soils.

APPENDIX 1

Some terms used in the governing finite element equations (equations (1) and (2)) are defined here.

Stiffness matrix **K**

$$\mathbf{K} = \int_V \mathbf{B}^T \mathbf{D} \mathbf{B} \, dV \tag{11}$$

Coupling matrix **L**

$$\mathbf{L} = \int_V \boldsymbol{a}\mathbf{d}^T \, dV \tag{12}$$

Flow matrix **Φ**

$$\mathbf{\Phi} = \int_V \mathbf{E}^T \mathbf{k} \mathbf{E} \, dV \tag{13}$$

Load vector $\Delta \boldsymbol{f}^{(i)}$

$$\Delta \boldsymbol{f}^{(i)} = \int_V \mathbf{N}^T \Delta \boldsymbol{F}^{(i)} \, dV + \int_S \mathbf{N}^T \Delta \boldsymbol{T}^{(i)} \, dS \tag{14}$$

Matrix for the imposed flow $\mathbf{G}^{FS}$

$$\mathbf{G}^{FS} = \int_\Gamma \boldsymbol{a}\boldsymbol{a}^T S_y \cos \beta \, d\Gamma \tag{15}$$

The matrices and vectors **B**, **D**, $\boldsymbol{a}$, $\boldsymbol{d}$, **E**, **k**, **N**, $\boldsymbol{F}$ and $\boldsymbol{T}$ and the scalars S_y and β are defined in the Notation.

NOTATION

- $\boldsymbol{a}$ vector of shape functions
- **B** displacement–strain matrix
- $\boldsymbol{d}$ vector relating nodal displacement to volumetric strain
- **D** stress–strain matrix
- d_h^* drawdown of the water table
- d_s surface subsidence
- **E** matrix relating the nodal total water head to ∇h^*
- E' Young's modulus
- $\boldsymbol{f}$ vector of body forces and surface tractions
- $\boldsymbol{F}$ vector of body forces
- G elastic shear modulus
- $\mathbf{G}^{FS}$ matrix for the imposed flow across the free surface
- h embedded depth of the sink point
- H thickness of the soil deposit
- h_{EL} elevation head
- h^* total water head
- $\boldsymbol{h}^*$ vector of total water heads
- i iteration number
- k permeability of a soil
- **k** matrix of permeability coefficients
- **K** stiffness matrix
- k_{limit} limit permeability for a soil
- k_n permeability normal to the free surface
- k_s permeability of a saturated soil
- **L** coupling matrix
- m number of nodes of an element
- n direction normal to a surface
- **N** matrix of element shape functions
- N_j shape function for the head at node j
- p excess pore-water pressure
- P pore-water pressure
- P_{limit} limit negative pore pressure for a soil
- Q pumping rate (volume per unit time)
- $\boldsymbol{Q}$ vector of pumping rates
- r polar co-ordinate
- r_{max} maximum radius
- S surface loaded by tractions, surface settlement
- S_0 long-term surface settlement immediately above the sink at $r = 0$)

S_y specific yield
t time
$\boldsymbol{T}$ vector of surface tractions
T_d time factor for drawdown of the water table
T_v time factor for surface subidence
V volume of the soil mass
x, y global Cartesian co-ordinates
z polar co-ordinate
α time marching integration factor
β angle between free surface segment and horizontal direction
Γ free surface contour
γ_w unit weight of water
δ displacement
$\boldsymbol{\delta}$ vector of nodal displacements
η local co-ordinate
ν' Poisson's ratio
ξ local co-ordinate
$\boldsymbol{\Phi}$ flow matrix
∇ vector operator $= [\partial/\partial x, \partial/\partial y, \partial/\partial z]^T$

REFERENCES

Bathe, K. J., Sonnad, V. & Domigan, P. (1982). Some experiences using finite element methods for fluid flow problems. *Proc. 4th Int. Conf. Finite Element Meth. Wat. Resour., Hanover*, 9.3–9.16.

Biot, M. A. (1941). General theory of three-dimensional consolidation. *J. Appl. Phys.* **12,** 155–164.

Biot, M. A. (1956). General solutions of the equations of elasticity and consolidation for a porous material. *J. Appl. Mech.* **23,** 91–96.

Booker, J. R. & Carter, J. P. (1984). Consolidation of a saturated elastic half space due to fluid extraction from a point sink. *Proceedings of the Engineering Foundation international conference on compressibility phenomena in subsidence, New Hampshire* (ed. S. K. Saxena), pp. 31–64. New York: Engineering Foundation.

Booker, J. R. & Carter, J. P. (1986a). Long term subsidence due to fluid extraction from a saturated anisotropic, elastic soil mass. *Q. J. Mech. Appl. Math.* **39,** Part 1, 85–97.

Booker, J. R. & Carter, J. P. (1986b). Analysis of a point sink embedded in a porous elastic half space. *Int. J. Numer. Anal. Meth. Geomech.* **10,** 137–150.

Booker, J. R. & Carter, J. P. (1987). Elastic consolidation around a point sink embedded in a half-space with anisotropic permeability. *Int. J. Numer. Anal. Methods Geomech.* **11,** 61–77.

Booker, J. R., Carter, J. P. & Small, J. C. (1985). Prediction of subsidence caused by pumping of groundwater. *Proc. 21st Congr. Int. Ass. Hydrau. Res., Melbourne*, 129–134.

Bouwer, H. (1964). Unsaturated flow in ground-water hydraulics. *J. Hydraul. Div. Am. Soc. Civ. Engrs* **90,** HY5, 121–144.

Cathie, D. N. & Dungar, R. (1975). The influence of the pressure–permeability relationship on the stability of a rock-filled dam. *Proceedings of international symposium on criteria and assumptions for numerical analysis of dams, Swansea*, pp. 830–845.

Christian, J. T. & Boehmer, J. W. (1970). Plane strain consolidation by finite elements. *J. Soil Mech. Fdn Engng Am. Soc. Civ. Engrs* **96,** SM4, 1435–1457.

Debidin, F. & Lee, C. F. (1980). Groundwater and drawdown in a large earth excavation. *Can. Geotech. J.* **17,** 185–202.

Delfranche, A. P. (1978). Land subsidence versus head decline in Texas. In *Evaluation and prediction of subsidence* (ed. S. K. Saxena), pp. 320–331. New York: American Society of Civil Engineers.

Desai, C. S. (1976). Finite element residual schemes for unconfined flow. *Int. J. Numer. Methods Engng* **10,** 1415–1418.

Desai, C. S. & Li, G. C. (1983). A residual flow procedure and application for free surface flow in porous media. *Adv. Wat. Resour.* **6,** 27–35.

Freeze, R. A. (1971). Influence of the unsaturated flow domain on seepage through earth dams. *Wat. Resour. Res.* **7,** No. 4, 929–941.

Gambolati, G. & Freeze, R. A. (1973). Mathematical simulation of the subsidence of Venice, 1, theory. *Wat. Resour. Res.* **9,** No. 3, 721–733.

Gambolati, G., Gatto, P. & Freeze, R. A. (1974). Mathematical simulation of the subsidence of Venice, 2, results. *Wat. Resour. Res.* **10,** No. 3, 563–577.

Harada, Y. & Yamanouchi, T. (1983). Land subsidence in Saga Plain, Japan and its analysis by the quasi three-dimensional aquifer model. *Geotech. Engng* **14,** No. 1, 23–54.

Herbert, R. (1968). Time variant ground water flow by resistance network analogues. *J. Hydrol.* **6,** 237–264.

Hsi, J. P. (1992). *Analysis of excavation involving drawdown of the water table.* PhD thesis, University of Sydney.

Hsi, J. P. & Small, J. C. (1992a). Ground settlements and drawdown of the water table around an excavation. *Can. Geotech. J.* **29,** No. 5, 740–756.

Hsi, J. P. & Small, J. C. (1992b). Simulation of excavation in a poro-elastic material. *Int. J. Numer. Anal. Meth. Geomech.* **16,** 25–43.

Hsi, J. P. & Small, J. C. (1992c). Analysis of excavation in an elasto-plastic soil involving drawdown of the water table. *Comput. Geotech.* **13,** 1–19.

Hsi, J. P. & Small, J. C. (1992d). Application of a fully coupled method to the analysis of an excavation. *Soils Fdns* **33,** No. 4.

Hwang, C. T., Morgenstern, N. R. & Murray, D. W. (1971). On solutions of plane strain consolidation problems by finite element methods. *Can. Geotech. J.* **8,** 109–118.

Kanok-Nukulchai, W. & Chau, K. T. (1990). Point sink fundamental solutions for subsidence prediction. *J. Engng Mech. Am. Soc. Civ. Engrs* **116,** No. 5, 1176–1182.

Neuman, S. P. & Witherspoon, P. A. (1971). Analysis of nonsteady flow with a free surface using the finite element method. *Wat. Resour. Res.* **7,** 611–623.

Premchitt, J. (1979). Land subsidence in Bangkok, Thailand: results of initial investigation, 1978. *Geotech. Engng* **10,** No. 1, 49–76.

Rushton, K. R. & Redshaw, S. C. (1979). *Seepage and groundwater flow, numerical analysis by analog and digital methods.* Chichester: Wiley.

Sandhu, R. S. & Wilson, E. L. (1969). Finite-element analysis of seepage in elastic media. *J. Engng Mech. Am. Soc. Civ. Engrs* **95,** EM3, 641–652.

Scott, R. F. (1978). Subsidence—a review. In *Evaluation and prediction of subsidence* (ed. S. K. Saxena). pp. 1–25. New York: American Society of Civil Engi-

neers.

Small, J. C. & Booker, J. R. (1984). Surface deformation of layered soil deposits due to extraction of water. *Proc. 9th Aust. Conf. Mech. Structs Mater., Sydney*, 33–38.

Small, J. C., Booker, J. R. & Davis, E. H. (1976). Elasto-plastic consolidation of soil. *Int. J. Solids Structs* **12**, 431–448.

Taipei Civil Engineers' Association (1985). *Evaluation of the ground settlement due to excavation and dewatering for the construction of Chung-Chow sewerage intake pump station in Kaoshung.* Project 8400TC. Taiwan: Taipei Civil Engineers' Association.

Taylor, G. S. & Luthin, J. N. (1969). Computer methods for transient analysis of water-table aquifers. *Wat. Resour. Res.* **5**, No. 1, 144–152.